

# Temperature-Dependent Refractive Index Determination from Critical Angle Measurements: Implications for Quantitative SPR Sensing

James H. Grassi and Rosina M. Georgiadis\*

Department of Chemistry, Boston University, Boston Massachusetts 02215

**Temperature-dependent measurements of surface coverage and interfacial kinetics remain relatively unexploited in thin-film sensing applications that rely on optical surface-sensitive techniques such as surface plasmon resonance spectroscopy (SPR). These techniques are inherently sensitive to the optical properties of the bulk solution in contact with the thin film; therefore, quantitative thin-film sensing requires accurate refractive index data for bulk solutions at the conditions of interest. The refractive index for bulk solutions depends strongly on temperature, solution composition, and optical excitation wavelength. In this paper, we demonstrate the use of critical angle measurements for accurate, independent determination of the refractive index of bulk solutions and present results for different experimental conditions of solution temperature, solution concentration, and excitation wavelength. We also examine the implications of incorrect accounting of the bulk solution for the case of two-color SPR sensing of ultrathin organic films. This sensing technique, which depends inherently on the contrast in the dispersion of the refractive index of the film and the bulk solution, can be over 1 order of magnitude more sensitive than single-color SPR measurements. Critical angle measurements can be implemented in conjunction with SPR measurements and will be invaluable for thin film sensing application in which the bulk refractive index varies during the experiment, for example, in temperature-dependent SPR measurements, or for applications in which the solution refractive index is not known.**

Measurements of the refractive index of bulk liquid solutions are important in many industrial and research applications including industrial process monitoring and chemical separation detectors. In recent years, accurate refractive index measurements have become increasingly important in chemical sensor<sup>1</sup> and biosensor<sup>2</sup> applications particularly in optical sensors based on evanescent wave techniques such as surface plasmon resonance (SPR) spectroscopy. These techniques, which can detect very low

levels of chemical and biological materials in real time without requiring analyte labeling, are sensitive to refractive index changes at the solid/solution interface in the environment immediately adjacent to the sensor surface. Characterization of the mass or thickness of ultrathin organic films via SPR sensing<sup>3,4</sup> is a versatile analytical approach, which is finding broad applications in biomedical, biomaterial, environmental, and agricultural research.

Although the SPR sensor response is extremely sensitive to selective molecular events at the sensor surface, any change in the refractive index of the medium within the evanescent field will affect the measurement. Variations in the refractive index arising from changes in bulk solution concentration or temperature may dominate the response if not accounted for properly.<sup>2</sup> These phenomena are sometimes referred to as “bulk effect” baseline shift or baseline drift and can result in large changes in the SPR signal that are not related to thickness changes of the adsorbed thin film. In some cases, it may be difficult to distinguish the sensor response due to selective surface binding from the response arising from bulk solution effects.

In the first part of this paper, we present an experimental approach for measuring the refractive index of bulk solutions. The method is based on analysis of the critical angle region of the angular reflectance spectrum and can be implemented simultaneously with SPR reflectance measurements. We demonstrate the feasibility of this approach for accurate measurement of the temperature dependence of bulk solution refractive indexes and compare our data with published literature values. For commonly used liquids, the temperature dependence of the refractive index is sufficiently strong ( $10^{-4}$ – $10^{-5}/^{\circ}\text{C}$ ) that temperature fluctuations can be a major source of error in SPR measurements.<sup>3</sup> A convenient way to minimize these errors is to record the temperature and account for the temperature fluctuations; however, the temperature dependence of the refractive index for the bulk solution must be known accurately. This information is also crucial for some of the most powerful emerging applications of SPR in which thermodynamic data can be extracted from temperature-dependent surface coverage measurements.<sup>5</sup> Accurate SPR measurements of the temperature dependence of equilibrium binding constants and reaction rate constants for chemical

\* To whom correspondence should be addressed: (e-mail) rgeorgia@bu.edu.

(1) Janata, J. *Principles of Chemical Sensors*; Modern Analytical Chemistry Series; Plenum Press: New York, 1989.  
(2) Davies, J. In *Surface Analytical Techniques for Probing Biomaterial Processes*; Davies, J., Ed.; CRC Press: Boca Raton, FL, 1996.

(3) Peterlinz, K. A.; Georgiadis, R. *Langmuir* **1996**, *12*, 4731–4740.

(4) Frutos, A. G.; Corn, R. M. *Anal. Chem. News Features* **1998**, *70*, A449–A455.

(5) Peterlinz, K. A.; Georgiadis, R.; Herne, T. M.; Tarlov, M. J. *J. Am. Chem. Soc.* **1997**, *119*, 3401–3402.

reactions at solid/liquid interfaces will have a potentially large impact on biosensor-based research in biochemistry and molecular biology as well as in other applications of surface analytical chemistry.

In the second part of this paper, we consider how an error in the assumed value in the bulk solution refractive index contributes to the overall uncertainty in SPR sensing of thin-film thickness. Our error analysis is concerned with two-color SPR,<sup>6</sup> a technique that is intrinsically sensitive to the relative dispersion of the adsorbed film and bulk solution. This method, developed in our laboratory for quantitative measurements of surface coverage of thin films at gold and other metal surfaces, can be more than 1 order of magnitude more sensitive than single-color methods.<sup>7,8</sup>

## EXPERIMENTAL SECTION

All refractive index data were obtained from analysis of critical angle reflectance data. Reflectance in the critical angle region was measured with an instrument designed for SPR measurements which incorporates a  $\theta/2\theta$  goniometer with  $0.001^\circ$  rotational precision and has been described previously.<sup>3</sup> Critical angle reflectance measurements were made as a function of angle of incidence at  $0.01^\circ$  intervals for 543.5- and 632.8-nm excitation. The TM (p-polarized) outputs of two He-Ne lasers directed along the same optical path were focused slightly to compensate for divergence. For all the data presented, solutions were held in an all-Teflon solution cell in contact with a hemispherical prism (BK7). Higher refractive index prisms are used for critical angle measurements made in conjunction with SPR reflectance.

The temperature in the solution cell was maintained by continuously circulating the solution through a programmable water bath in which the temperature is controlled to  $0.01^\circ\text{C}$ . A peristaltic pump circulates the solution through the cell at a rate of  $\sim 20$  mL/min. The temperature in the solution cell (measured by a Teflon-coated thermocouple) is stable to  $0.05^\circ\text{C}$  over the course of a full critical angle scan. This variation in temperature corresponds to an uncertainty of  $\sim 5 \times 10^{-6}$  in the refractive index of water at room temperature. Several critical angle scans were collected at each temperature. All solutions used Nanopure water (Barnstead E-pure, 18 MW) and high-purity salts, NaCl (Fisher), NaClO<sub>4</sub> (Fisher), and KH<sub>2</sub>PO<sub>4</sub> (Aldrich).

## RESULTS AND DISCUSSION

### Temperature-Dependent Critical Angle Measurements.

Highly accurate temperature-dependent refractive index data for liquid solutions are compiled in reference tables for many for pure liquids and many solutions.<sup>9</sup> If data are available for the *specific* solution of interest, the temperature dependence or concentration dependence of the refractive index can be estimated by interpolation from empirical fits to the available data. However, it is difficult to estimate the refractive index for a *different* material, concentration, or temperature by extrapolation or by using generalized models.<sup>10</sup> For example, for many liquids, values of the refractive index predicted by the general Lorentz-Lorenz formula are

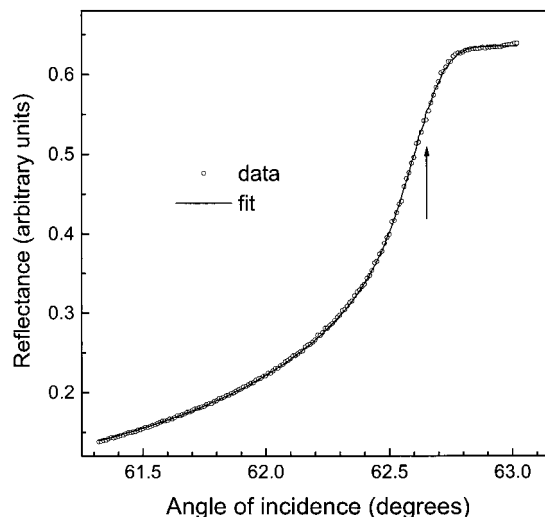


Figure 1. Reflectance near the critical angle for 1.0 M KH<sub>2</sub>PO<sub>4</sub> at 543.5 nm. Shown are the reflectance data (open circles) as a function of angle of the incidence and best fit to the data using a two-layer Fresnel reflectance model (solid line); see text for details. The angle of incidence is calibrated relative to a reference critical angle for water. The critical angle,  $\theta_{\text{critical}} = 62.650^\circ$ , is shown by the vertical arrow.

accurate to only a few percent.<sup>11</sup> Accurate theoretical predictions are difficult because the density of a liquid solution is not a simple function of temperature and concentration; attempts to use theoretical physical models to modify the Lorentz-Lorenz formula for liquids<sup>12</sup> have had limited validity. Therefore, experimental measurements are needed in many cases.<sup>13</sup>

Figure 1 shows a representative critical angle scan as a function of angle of incidence and the fit to the data. The data, obtained for a solution of 1.0 M KH<sub>2</sub>PO<sub>4</sub>, show the expected sharp change in optical reflectance near the critical angle. All critical angle reflectance scans were analyzed by fitting the data to a Fresnel model (solid line in Figure 1). The theoretical model used to fit the data is convoluted with the experimental instrument function to account for the finite width of the laser beam profile. For all solutions and temperatures studied, the data are fit well by this model; fit residuals are typically on the order of 0.001. The resulting error in the bulk solution refractive index determined from fitting an individual critical angle scan (200 angular measurements) is less than one part in the sixth decimal place. All refractive index data were measured relative to the reference values for  $20^\circ\text{C}$  water<sup>14</sup> of  $n_o(632.8\text{ nm}) = 1.331745$  and  $n_o(543.5\text{ nm}) = 1.33461$ . Before each measurement, the angle of incidence of the instrument was calibrated by measuring critical angle scans for water at both 632.8- and 543.5-nm excitation.

The temperature dependence of the bulk solution refractive index,  $n_s(T)$ , was measured at a range of concentrations for various aqueous salt solutions (see Table 1) and for a number of nonaqueous solutions (not shown). Water was used as a standard, the data are in excellent agreement with the literature.<sup>14</sup> Typical data showing the temperature dependence of the refractive index

(6) Peterlinz, K. A.; Georgiadis, R. *Opt. Commun.* **1996**, *130*, 260–266.

(7) Peterlinz, K. A.; Georgiadis, R. *J. Phys. Chem.* **1997**, *101*, 8041.

(8) Chinowsky, T. M.; Yee, S. *Sens. Actuators B* **1998**, *51* (1–3), 321–330.

(9) *CRC Handbook of Chemistry and Physics*; CRC Press: Boston, 1990.

(10) Lu, W.; Worek, W. M. *Appl. Opt.* **1993**, *32*, 3992–4002.

(11) Beysens, D.; Calmettes, P. *J. Chem. Phys.* **1977**, *66*, 766–771.

(12) Proutiere, A.; Megnassan, E.; Hueteau, H. *J. Phys. Chem.* **1992**, *96*, 3485–3489.

(13) Hanning, A.; Roeraade, J. *Anal. Chem.* **1997**, *69*, 1496–1503.

(14) Harvey, A. H.; Gallagher, J. S.; Sengers, J. M. H. L. *J. Phys. Chem. Ref. Data* **1998**, *27*, 761–774 and references therein.

Table 1. Temperature Dependence of the Solution Refractive Index  $n_s$  Relative to  $n_o^a$

solution	M	632.8 nm		543.5 nm	
		$-A (\times 10^{-5})$	$-B (\times 10^{-7})$	$-A (\times 10^{-5})$	$-B (\times 10^{-7})$
H <sub>2</sub> O		8.5	10.0	8.8	14.3
NaClO <sub>4</sub>	1.0	13.6	8.0	13.9	10.0
	0.5	12.2	10.0	12.0	13.0
	0.1	9.4	10.0	10.0	12.0
NaCl	1.0	10.1	8.0	10.7	9.0
	0.5	9.6	11.0	10.2	11.0
	0.1	9.0	12.0	9.0	15.0
KH <sub>2</sub> PO <sub>4</sub>	1.0	10.6	8.0	10.6	12.0
	0.5	9.8	7.0	9.8	10.0
	0.1	8.7	10.0	8.6	11.0

<sup>a</sup>  $A$  and  $B$  are parameters in the equation,  $n_s - n_o = A(t - 20) + B(t - 20)^2$  for  $13^\circ\text{C} < t < 31^\circ\text{C}$ . The tabulated values represent the best fit to the experimentally measured relative refractive index data as a function of temperature for the solution composition and concentration indicated. All refractive index data are obtained from analysis of critical angle data at the wavelengths indicated. All measurements relative to water at  $20^\circ\text{C}$ ,  $n_o$ , see text.

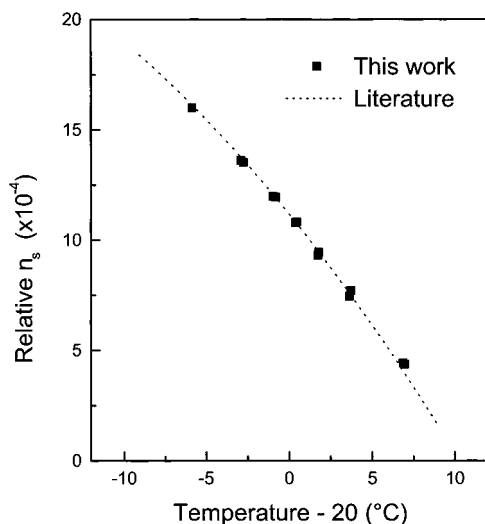


Figure 2. Temperature dependence of the refractive index for 0.1 M NaCl. The data, obtained from critical angle measurements, are plotted relative to the refractive index of water,  $n_o$ , at  $20^\circ\text{C}$ . The dotted line shows the comparison with literature data from ref 10 plotted on the same relative scale. The temperature dependence of the refractive index is fit to a second-order polynomial (not shown). Fitting parameters (coefficients to the second-order polynomial) are tabulated in Table 1 for several concentrations and electrolytes.

for an aqueous solution are given in Figure 2. The data, shown here for 0.1 M NaCl at 632.8 nm, are plotted relative to the refractive index of water at  $20^\circ\text{C}$ . The temperature dependence can be fit to a second-order polynomial; see Table 1 for fitting parameters. Our results are in very good agreement with the literature.<sup>10</sup> All solutions showed the expected behavior: (1) the refractive indexes decrease with increasing temperature; (2) the falloff becomes progressively stronger as the temperature rises although the detailed behavior (slope and curvature) depends strongly on solution concentration and composition.

**Implications for SPR Sensing.** In this section, we consider how an error in the solution dielectric constant contributes to the error in the thickness of an ultrathin organic film determined by two-color SPR sensing. In our analysis, we consider the intrinsic

error incurred by incorrect assumptions in the *data analysis* rather than the error associated with measurement noise. Typically, SPR data analysis is based on a modified Fresnel reflectivity model for  $N$  layers; here four layers are considered (prism/metal/thin film/solvent). Not surprisingly, the overall uncertainty in SPR sensing of thin dielectric films is highest for the thinnest films and is reduced considerably if the optical parameters for all *other* layers, including those for the substrate and solution, are known. The prism refractive index is well characterized; the optical constants of the metal layer can be determined from detailed fitting analysis and control experiments.<sup>15</sup> If the solvent index is known, the only remaining unknowns are the parameters of interest: the thickness and dielectric constant of the thin film. For transparent films, the dielectric constant is equal to the square of the refractive index ( $\epsilon_f = n_f^2$ ).

As we will see, independent accurate knowledge of the solution refractive index from critical angle measurements can significantly reduce the uncertainty in accurate quantitative SPR sensing of ultrathin organic films. We focus on systems involving these ultrathin dielectric films ( $<10$  nm thickness) because of the importance of quantitative measurements in this regime, for example, for monitoring the kinetics of the initial stages of adsorption and film formation.<sup>3</sup> However, the same effects should be important in many other surface plasmon methods and their application even for much thicker films. For experiments involving low ligand density or for small-molecule interactions, the measured changes in the SPR response are equivalent to the determination of the effective thickness of an ultrathin dielectric film layer in the presence of buffer solution. Therefore, the approaches for quantitative measurements outlined here can be applied more generally to extract accurate surface coverage for surface/ligand or receptor/ligand interactions from equilibrium SPR data or SPR kinetics studies.<sup>16</sup>

There are several approaches for extracting information about thin dielectric films from SPR data. The most common approach involves extracting the values for the two unknown thin film parameters, the film thickness ( $d_f$ ) and the film dielectric constant ( $\epsilon_f$ ), from analysis of angle of incidence modulated data obtained at a particular excitation wavelength (single-color SPR). For thin films, any number of different combinations of  $d_f$  and  $\epsilon_f$  may be found to fit the reflectance data. Consequently, thin-film thicknesses determined from a single measurement have high uncertainty.<sup>6,7</sup> Most researchers resort to assuming a fixed value for the film dielectric constant on the basis of the known chemical properties of the film. The best-fit value for the thickness of the thin film can be determined from fitting analysis of the measured reflectance data to a multilayer optical reflectance model in which all other optical parameters are held fixed at assumed values. If these assumptions are valid, relative film thickness information can be obtained from the analysis of single wavelength data. This is similar to the assumption that, within a family of similar compounds, that the relative change in the minimum reflectance is proportional to the mass of adsorbed material.

We<sup>3,6</sup> and others<sup>15</sup> have shown that alternative approaches can provide independent determination of both unknown thin-film

(15) Bruijn, H. E. d.; Altenburg, B. S. F.; Kooyman, R. P. H.; Greve, J. *Opt. Commun.* **1991**, *82*, 425–432.

(16) Winzor, D. J.; Sawyer, W. H. *Quantitative Characterization of Ligand Binding*; John Wiley: New York, 1995.

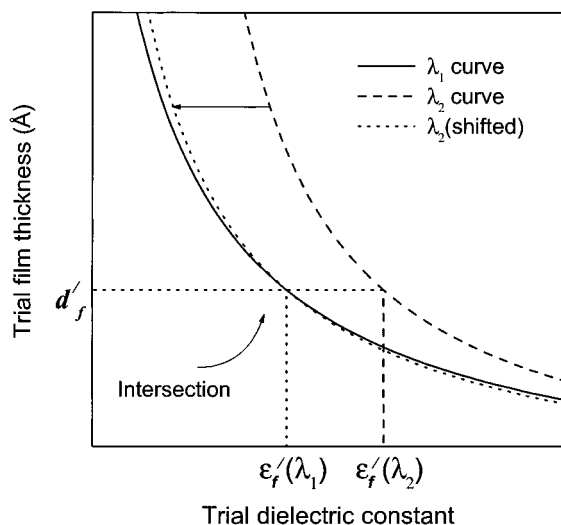


Figure 3. Illustration of the two-color SPR approach for determining thickness and dielectric constants for a thin film. Shown are the trial film thickness versus trial dielectric constant that equally well describes the SPR reflectance data sets for two excitation wavelengths,  $\lambda_1$  (solid curve) and  $\lambda_2$  (dashed curve). Accounting for the dispersion of the thin-film layer results in a shifted trial curve for  $\lambda_2$  (dashed curve). The intersection point indicates the true thickness and dielectric constant (at  $\lambda_1$ ).

parameters,  $d_f$  and  $\epsilon_f$ . These methods require analysis of additional data obtained under a different condition, such as data obtained at second excitation wavelength. In the two-color SPR approach,<sup>6</sup> independent estimates of the values of the film thickness and dielectric constant are obtained from the intersection point of the two trial curves ( $d_f, \epsilon_f$ ) <sub>$\lambda_1$</sub>  and ( $d_f, \epsilon_f$ ) <sub>$\lambda_2$</sub> , see Figure 3. For each excitation wavelength, the trial curve represents all combinations of  $d_f$  and  $\epsilon_f$  that fit the reflectance data obtained at that wavelength. For example, a combination in which  $d_f$  is large and  $\epsilon_f$  is small can fit the reflectance data equally well as another in which  $d_f$  is small and  $\epsilon_f$  is large. The intersection of the two trial curves (corrected for the dispersion of the film<sup>6</sup>) represents the unique pair of parameters ( $d_f, \epsilon_f$ ) that are consistent with the experimental reflectance data at both wavelengths. Single-wavelength analysis will not be considered in detail here. The overall uncertainty in determining  $d_f$  for thin films (without prior independent knowledge of  $\epsilon_f$ ) is large under typical experimental conditions<sup>8</sup> and overshadows the error due to incorrect accounting of the solution refractive index.

To address the inherent error associated with incorrect accounting of the bulk solution in data analysis, our error analysis calculations use simulated (noise-free) SPR data. Parameters are typical<sup>6</sup> for a four-layer system consisting of an aliphatic organic monolayer film on gold in contact with an organic solvent, water, or aqueous electrolyte solution. For the data presented in Table 2, the model is for an aliphatic film (nominal thickness  $d_{f,N} = 4.0$  nm) adsorbed on gold in contact with an organic solvent (ethanol). A four-layer modified Fresnel optical model was used to account for the prism, metal, film, and solution layers. At 632.8-nm excitation, the dielectric constants used in the model were 2.969 03,  $-11.5941 + i2.4259$ , 2.1000, and 1.846 31, respectively. At 543.5-nm excitation, the dielectric constants used in the model were 3.009 28,  $-6 + i2.4259$ , 2.1080, and 1.854 01, respectively. Calculations were performed for different values of the thin-film

Table 2. Fractional Error,  $(d_f' - d_f)/d_f$ , in Film Thickness,  $d_f$ , Calculated from Two-Color SPR Analysis When the Solution Dielectric Constant Is Underestimated by  $\Delta\epsilon_s$ <sup>a</sup>

$d_f =$ 4.0 nm		$\Delta\epsilon_s(632.8 \text{ nm}) (\times 10^{-5})$			
		0	1	2	5
$\Delta\epsilon_s(543.5 \text{ nm}) (\times 10^{-5})$	0	0.00	0.05	0.10	0.27
	1	-0.03	0.02	0.07	0.23
	2	-0.06	-0.01	0.03	0.19
	5	-0.14	-0.10	-0.06	0.09

<sup>a</sup> The fractional error,  $(d_f' - d_f)/d_f$ , in the calculated thin film thickness,  $d_f$ , due to assuming an incorrect value of  $\epsilon_s$  for the solution layer. The fractional error is determined by comparing the nominal film thickness,  $d_f$ , with the result calculated from the crossing point ( $d_f, \epsilon_f$ ) of two trial curves. The trial curves are obtained from two-color analysis of simulated SPR reflectance curves at 632.8- and 543.5-nm excitation using an optical model that assumes the nominal parameters for the thin film ( $d_f = 4.0$  nm;  $\epsilon_f = 2.1$  (at 632.8 nm)) but assumes an *incorrect*, fixed value for  $\epsilon_s = \epsilon_s + \Delta\epsilon_s$  for the solution layer (nominal value of  $\epsilon_s = 1.84631$ ). The lowest fractional error, along the shaded diagonal, corresponds to the case where the dispersion relation for the solution dielectric constant ( $\epsilon_s(632.8 \text{ nm}) - \epsilon_s(543.5 \text{ nm})$ ) is maintained constant at nominal value of 0.008 during the analysis.

thickness less than 10 nm as well as for various different solutions. The metal film thickness was 45.9 nm for all calculations.

In all cases studied, incorrect accounting of the bulk solution results in a trial curve of significantly different *shape*. For example, if  $\epsilon_s$  is underestimated in the SPR data analysis, the trial curve shifts to higher values of  $d_f$  to compensate. Since the thickness and dielectric constant are coupled,  $d_f$  will compensate more for smaller values of  $\epsilon_f$ , creating a new trial curve of altered shape. Since  $d_f$  and  $\epsilon_f$  are obtained from the intersection point of two trial curves, correct error analysis must consider error contributions from both trial curves. These contributions are generally not the same; for a given  $\Delta\epsilon_s$ , the trial curve for  $\lambda = 632.8$  nm shows a larger shift than the trial curve for  $\lambda = 543.5$  nm. This is related to the fact that  $\epsilon_s$  increases monotonically with decreasing wavelength.

Tabulated in Table 2 is the fractional error for determining the correct value of the film thickness,  $d_f$ , for a given uncertainty ( $\Delta\epsilon_s$ ) in the assumed value of  $\epsilon_s$ . The fractional error is determined by comparing the nominal film thickness,  $d_{f,N} = 4.0$  nm, with the thickness calculated from the crossing point ( $d_f, \epsilon_f$ ) of trial curves obtained from two-color analysis of simulated SPR reflectance curves. The trial curves at 632.8- and 543.5-nm excitation are generated using an optical model that assumes an *incorrect* fixed value for  $\epsilon_s = \epsilon_{s,N} - \Delta\epsilon_s$  for the solution layer (nominal value of  $\epsilon_{s,N}(632.8 \text{ nm}) = 1.84631$ ). The lowest fractional error, along the shaded diagonal in Table 2, corresponds to the case where the dispersion relation for the solution dielectric constant ( $\epsilon_s(632.8 \text{ nm}) - \epsilon_s(543.5 \text{ nm})$ ) is maintained constant at 0.008 in the analysis. For a particular film thickness, the fractional error in  $d_f$

increases linearly as the error in  $\Delta\epsilon_s$  increases. Not surprisingly, the contribution of error  $\Delta\epsilon_s$  to the intrinsic error in  $d_f$  is much larger for the thinnest films; for a given  $\Delta\epsilon_s$ , the fractional error in the resulting determination of  $d_f$  increases logarithmically with decreasing film thickness (not shown).

Chinowsky and co-workers have recently revisited the issue of quantifying the uncertainty in film parameter determination from SPR reflectivity data.<sup>8</sup> In trying to quantify the relative uncertainty in SPR sensing, Chinowsky and co-workers have considered only the fundamental limitation imposed by *measurement noise* and do not take into account additional errors, such as those incurred by assumptions in the data analysis. Even so, their results suggest that certain assumptions in data analysis are likely to be important. They found that, for two-color analysis of equally noisy data, higher *contrast* between the dispersion of the thin film and the buffer appears to correlate with lower overall uncertainty in determining  $d_f$  independent of  $\epsilon'_f$ . They also confirmed that, for thin films of <10 nm,  $d_f$  can be estimated independently of  $\epsilon_f$  from single-wavelength analysis but only with large uncertainty:<sup>7</sup> the uncertainty in single-color thin film sensing can be over 1 order of magnitude greater than that obtained by a two-color approach.

These observations are in general agreement with our results. In our analysis, we considered films of varying thickness (2.0, 4.0, and 8.0 nm) in a variety of aqueous and nonaqueous solvents. Some general trends were observed for all cases. First, when the nominal dispersion relation for the solvent was maintained, the uncertainty in  $d_f$  was found to vary linearly with  $\Delta\epsilon_s$  for small values of  $\Delta\epsilon_s$  ( $\leq 0.0001$ ). Larger values of  $\Delta\epsilon_s$  were not considered in our analysis because it is difficult to find a reasonable intersection point for the trial curves. Second, the error in determining  $d_f$  was smallest if the dispersion relation for the solution was correct (along the diagonal in Table 2) and increased slowly with  $\Delta\epsilon_s$ . If the dispersion relation was not maintained, the overall uncertainty in  $d_f$  increased very steeply with increasing  $\Delta\epsilon_s$  (off-diagonal entries in Table 2). Third, the sensitivity of the two-color method depended in a complex way on the relative dispersion of the film and buffer, the ratio of slopes, and shape of the ( $d_f$ ,  $\epsilon'_f$ ) curves near the crossing point.<sup>6</sup> Therefore, quantitative calculations to determine the sensitivity of the technique or the contribution of errors are valid only for the specific film conditions modeled. For example, choice of solution can be very important. For the errors given in Table 2, the solvent was ethanol. When the calculations are repeated for the same film in contact with water or dilute aqueous electrolyte solution, the error contributions to  $d_f$  drop by a factor of 3. Finally, in a related aspect, the *contrast*

between the dispersion in the refractive index of the thin film and the dispersion in the refractive index of the solvent is important. For the results in Table 2, the solvent dispersion is equal to the dispersion in the film representing the worst-case scenario.

Regardless of these details of how errors in  $d_f$  and  $\epsilon'_f$  depend on the optical constants of the particular interface of interest, it is always true that any uncertainty in the refractive index of the bulk solution leads to a higher overall error. As we have shown, the resulting error can be larger than the error associated with measurement noise in some cases. Critical angle measurements provide important supporting information regarding the refractive index of the bulk solution which can be used in SPR data analysis to improve the accuracy of SPR sensing.

## CONCLUSIONS

In this paper, we demonstrate the use of critical angle measurements for accurate determination of the refractive index of bulk solutions and present results for different experimental conditions of temperature, solution concentration, and excitation wavelength. These measurements, which can be performed in conjunction with SPR, are invaluable for quantitative thin-film sensing applications where the bulk refractive index varies during the experiment, as in temperature-dependent measurements, and for other applications in which it may not be possible to estimate the solution dielectric constant with sufficient accuracy. The ability to make reliable critical angle measurements has important implications for sensing of ultrathin films by two-color SPR, a quantitative surface analytical technique that can be over 1 order of magnitude more sensitive than single-color SPR. When the bulk solution is correctly accounted for in two-color SPR data analysis, accurate quantitative thin-film sensing can be achieved. While we have concentrated on demonstrating these methodologies and presenting error analysis results for extremely thin films of <10 nm, the same effects should be important in many surface plasmon methods and their applications.

## ACKNOWLEDGMENT

We thank Mr. Jacob Krich for help with data collection and Dr. Kevin Peterlinz for help with experimental aspects and for helpful discussions. We gratefully acknowledge the support of the National Science Foundation (Grant CHE-9502757).

Received for review February 5, 1999. Accepted July 19, 1999.

AC990125Q